Modelling and Optimization of Modular System for Power Generation from a Salinity Gradient

Ali Altaee[1], Andrea Cippolina[2]

[1]School of Civil and Environmental Engineering, University of Technology Sydney, 13 Broadway, Ultimo, NSW 2007, Australia. Email: ali.altaee@uts.edu.au; Tel: +61295149668

[2] Dipartimento di Ingegneria, Università degli Studi di Palermo, viale delle Scienze Ed.6, 90128 Palermo, Italy

Abstract

Pressure retarded osmosis has been proposed for power generation from a salinity gradient resource. The process has been promoted as a promising technology for power generation from renewable resources, but most of the experimental work has been done on a laboratory size units. To date, pressure retarded osmosis optimization and operation is based on parametric studies performed on laboratory scale units, which leaves a gap in our understanding of the process behaviour in a full-scale modular system. A computer model has been developed to predict the process performance. Process modelling was performed on a full-scale membrane module and impact of key operating parameters such as hydraulic feed pressure and feed and draw solution rates were evaluated. Results showed that the optimum fraction of feed/draw solution in a mixture is less than what has been earlier proposed ratio of 50% and it is entirely dependent on the salinity gradient resource concentration. Furthermore, the optimized pressure retarded osmosis process requires a hydraulic pressure less than that in the normal (unoptimized) process. The results here demonstrate that the energy output from the optimized pressure regarded osmosis process is up to 54% higher than that in the normal (unoptimized) process.

Keywords: Renewable energy, Pressure retarded osmosis, Membrane technology, Salinity gradient, Process optimization

1. Introduction:

Renewable energy resources have been profoundly investigated over time to provide an alternative source to fossil fuel energy and secure long-term increasing demands on energy [1, 2]. Amongst the emerging renewable energy technologies, salinity gradient power plant stands out as one of the most promising processes [3, 4]. Salinity gradient energy conversion can be achieved by pressure retarded osmosis (PRO) or reverse electrodialysis (RED) processes [2, 5, 6]. In the RED technology, selective anion and cation exchange membranes alternatively separate a concentrate and a dilute solution. Ions spontaneously move from the high to the low salinity solution compartment and, thanks to the presence of selective ion exchange membranes, this movement generates an electrical ionic current, which is converted

into a current of electrons in the two end electrodic compartments [7, 8]. At the same time, electro-chemical equilibria at the solutions/membranes interface generate a voltage increase along the same direction of electric current, thus reproducing the operation of a power generator or a battery.

Pressure retarded osmosis operates in a different way. The high and low concentration solutions are separated by an osmotic membrane that rejects ionic species but allows water to pass through from the dilute solution to the concentrate one, driven by the difference in water activity (i.e. in osmotic pressure) of the two solutions [8]. In PRO, the high concentration solution (draw solution) is pressurized and fed into the membrane module, so that the passage of water from the low salinity (feed) solution is "retarded" by the hydraulic pressure applied. In this way, the permeating water the gains pressure and the chemical potential is converted into pressure energy or hydraulic energy transferred to the draw solution. Fraction of the diluted draw solution equals to the volume of permeate flow goes into a hydro turbine for power generation while the other fraction is used to pressurize the draw solution entering the membrane module via an ideal pressure exchanger [figure 1].

Despite the high potential of salinity gradient power technologies, PRO technology has not been commercialized yet. Several pilot plants have been tested worldwide in addition to the large number of laboratory size experiments. First pilot plant was tested by Statkraft using the salinity gradient between seawater and river water, and was not successful to satisfy the required energy demands [3]. This is, most likely, because of the low osmotic pressure driving force across the PRO membrane [3]. Subsequent pilot plant test in Mega-ton project, Japan, demonstrated better results with 7.7 W/m^2 power density [9], that is greater than recommended threshold of 5.5 W/m^2 [3]. Toyobo hollow fiber membrane was used in the conjunction with the salinity gradient of reverse osmosis (RO) brine and wastewater for power generation. With Toyobo membrane, a maximum 30 bar feed pressure can be applied on the draw solution side of the PRO membrane [10]. However, researchers have developed laboratory scale membranes with high water flux and can tolerate a range of hydraulic pressure that exceeds 30 bar. Madsen et al., carried out PRO experiment at 70 bar using 5M NaCl draw solution to reach power density in excess of 5.5 W/m^2 [11]. Li et al., [12] reported 4.3 W/m^2 power density at 12 to 13 bar hydraulic pressure using wastewater RO retentate and 1M NaCl feed and draw solution, respectively. The research group used in-house developed hollow fiber PRO membrane and experiments were performed at Forward Osmosis (FO) mode [AL-FS] to decrease pretreatment requirements of feed solution. Wan and co-workers [13] achieved 38 W/m^2 at 30 bar hydraulic pressure using thin-film composite hollow fiber membrane. The salinity gradient resource was DI water feed solution and 1.2M NaCl draw solution. In an experiment to evaluate the structural stability of PRO membrane researchers conducted PRO experiment over 10 hours on a laboratory fabricated membrane polyamide membrane [14]. A power density of 12.8 W/m^2 was achieved at 17.2 bar hydraulic pressure. Chen et al., [15] performed a laboratory experiment to test stability of polyamide PRO membrane. The research group reported 19.2 W/m^2 power density at 15.0 bar hydraulic pressure using 1.0 M NaCl

and DI water as the draw and feed solution, respectively. Hickenbottom et al., [16] evaluated commercially available membrane for PRO process. The study found that thin-film composite (TFC) polyamide membrane from Hydration Technology Innovations (HTI) is the most stable membrane with 22.6 W/m^2 power density at 41 bar hydraulic pressure using 3M NaCl draw solution. Unfortunately, membrane deformation was detected at 35 bar hydraulic pressure.

In the unoptimized (normal) PRO process, the recommended hydraulic pressure is equal to $\Delta P = \Delta\pi/2$ and the flow rate of feed solution is equal to that of draw solution [4]. Most researchers and scientists still recommend optimum values of hydraulic pressure and feed to draw mixing ratio that are obtained from a laboratory scale PRO process, ignoring the difference in the hydrodynamic conditions and concentration variation along channels between laboratory and full-scale membrane [5, 17]. However, dilution and concentration of draw and feed solution in a full-scale PRO module affect the osmotic driving force and extractable energy along the PRO membrane. Tamburini et al. [18] reported a very preliminary analysis of the effect of up-scaling and non-ideal phenomena in PRO performance. The study highlighted the evidence that optimal operating pressure and flow rate may differ depending on module geometry and feed composition. However, in that study, no effort toward a structured optimisation process was performed.

In the current study, a computer model was applied to find the optimum hydraulic pressure and feed to draw ratio that is required to maximize the energy output from salinity gradient in the PRO process. The performance of the PRO process was optimized in a full-scale PRO module using a validated computer model. The study investigated different types of salinity gradients to mimic a number of natural feed and draw solutions that would have been suggested in the PRO process.

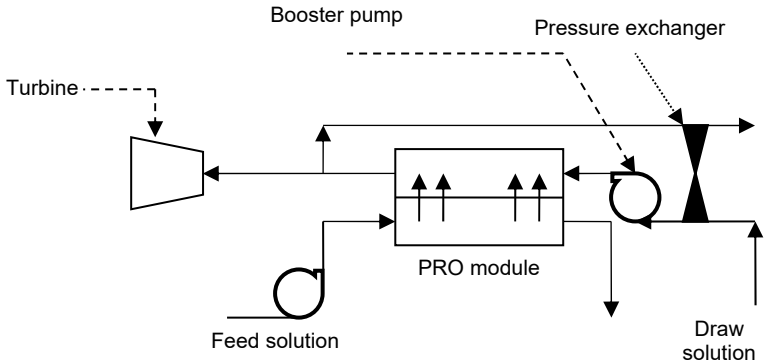

Figure 1: A schematic diagram of PRO process

2. Materials and methods

2.1 Pressure retarded osmosis model

A physical model was used to calculate water flux in the PRO process taking into account the impact of concentration polarization and external resistance along the PRO module. Some details on the model formulation and implementation are reported in the Appendix A1, while only the main equations are presented below. The model was validated using experimental data from a pilot plant [20], though relevant information is also reported in the Appendix A2 [Table A1]. Water flux along the PRO module was calculated from the following equation [17]:

$$J_{w,x} = A_w\left\{\frac{\left(nRTC_{Di,x}\left(1+\frac{Q_{Di,x}}{Q_{Do,x}}\right)/2\right)\exp\left(\frac{-J_{w,x}}{k_d}\right)-nRTC_{Fi,x}\left(1-\frac{Q_{Fi,x}}{Q_{Fo,x}}\right)\exp\left(J_{w,x}K+\frac{J_{w,x}}{k_f}\right)}{1+\frac{B}{J_{w,x}}\left(\exp\left(J_{w,x}\frac{J_{w,x}}{k_f}\right)-\exp\left(\frac{-J_{w,x}}{k_d}\right)\right)}-\Delta P\right\} \quad [1]$$

where, $J_{w,x}$ is the water flux (L/m^{2}h) along the PRO module with interval x = 0.1 m, n is number of ions in the solution, R is the gas constant, and T is the temperature in Kelvin. A_w and B were assumed to be 1.23 L/h.m^2·bar and 2.6 kg/h.m^2 respectively, k_d=k_f=0.18 m/h, and K=31 h/m, $C_{Di,x}$ represents the inlet concentration of the draw solution at the distance x along the membrane, $C_{Fi,x}$ represents the inlet concentration of the feed solution at the distance x along the membrane, $Q_{Di,x}$ and $Q_{Do,x}$ represent the inlet and outlet flow rate of the draw solution, respectively, and $Q_{Fi,x}$ and $Q_{Fo,x}$ represent the inlet and outlet flow rate of feed solution at distance x along the membrane, respectively [18]. In this study, the length of the PRO module is 1 m [17] and has 24 m^2 active area. Equation 1 accounts for concentration polarization and external resistance in the PRO membrane [9]. Equation 1 is valid for PRO membrane operating on the PRO mode; i.e. draw solution faces the active layer. More details on the model derivation can be found in the Appendix A1 and literature [17]. The fractions of draw and feed volumes, λ_D and λ_F respectively, in the mixture solution were calculated from the following equations:

$$\lambda_D = \frac{\gamma_D}{\gamma_D + \gamma_F} \quad [2]$$

$$\lambda_F = \frac{\gamma_F}{\gamma_F + \gamma_D} \quad [3]$$

where, γ_D and γ_F are the volumetric flow rates of draw and feed solution. Specific energy generation, Es (kWh/m^3), was calculated at different operating conditions using the following expression:

$$Es = \frac{\Delta P * Q_p}{Q_D + Q_F} \quad [4]$$

where, ΔP is the hydraulic pressure of the draw solution entering the hydro turbine (bar) and Q_p, Q_D and Q_F are the permeate, draw and feed solution flow rates, respectively. In this study, we performed PRO optimization to find the optimum hydraulic pressure and mixing ratios in the PRO system leading to maximum values of specific energy output (*Es*). Optimized values of *Es* were compared with those in the unoptimized (normal) PRO case for each salinity gradient resource considered. Matlab software was used to implement the model and the optimization algorithm of the PRO process.

3. Results

3.1 Applied hydraulic pressure optimization

Previous studies recommended the optimum hydraulic pressure for the power density to reach a maximum amount is $\Delta P = \Delta\pi / 2$ [4, 5]. This value has been experimentally validated on a flat sheet PRO unit as well as in a full scale ideal PRO process; i.e. ignoring the effect of concentration polarization [5]. We performed PRO optimization for a full-scale spiral wound module taking into account the impact of concentration polarization and results were compared with that from unoptimized PRO process. We assumed pressure drop along the spiral wound is insignificant. Four salinity gradient resources were evaluated using sodium chloride salt, these are 5M-0.6M, 5M-1.2M, 1.2M-0.02M and 0.6M-0.02M to resemble field situation of Dead Sea-seawater, Dead Sea-RO brine, RO brine-wastewater, and seawater-wastewater, respectively. These salinity gradients have been widely investigated in literature due to their potential for application in salinity gradient power plant [1, 5, 6].

Hydraulic pressure optimization was performed using equal feed and darw solution flow rates, 2000 L/h. Results in Figure 2A show hydraulic pressure in optimized and unoptimized PRO process consisting of one full-scale module. In general, hydraulic pressure was 5% to 14% lower in the optimized PRO compared to the unoptimized PRO process. The largest difference was 14% for 0.6M-0.02M salinity gradient followed by 7.5%, 5.5% and 11% for 5M-0.6M, 5M-1.2M and 1.2M-0.02M salinity gradients, respectively. Water flux in the PRO module is shown in Figure 2B. Optimized PRO processes exhibited higher water flux than unoptimized PRO processes because of the higher net driving force across the membrane. Water flux decreased across the PRO membrane due to osmotic pressure decrease as a result of dilution of the draw solution and concentration of the feed solution. Figure 2C shows the net energy output in the optimized and unoptimized PRO processes. Hydraulic pressure optimization resulted in none to subtle increase in the energy output in the PRO process. 5M-0.6M and 5M-1.2M salinity gradients exhibited 0.7% and 0.6% increase in energy generation due to the optimization of hydraulic pressure while 1.2M-0.02M and 0.6M-0.02M salinity gradients showed no improvement in the energy generation due to optimization of the hydraulic pressure.

The average power density in the optimized PRO process was calculated as the average membrane flux multiplied by the hydraulic pressure; i.e. $W_{ave}=J_{w\text{-}ave}*P$ [17]. Results show that the average power density of 5M-0.6M, 5M-1.2M and 1.2M-

0.02M salinity gradients was slightly higher in the optimized PRO compared to the unoptimized PRO process while there is no improvement in 0.6M-0.02M salinity gradient [Figure 2D]. Apart from 0.6M-0.02M salinity gradient, all salinity gradient resources achieved average power density over 5 W/m^2 threshold value that is recommended in the PRO process. The advantage of optimization was that optimized PRO process requires less pressure for operation. This would be reflected on the type and characteristics of PRO membrane and high pressure pump and, eventually, on the capital cost of the PRO plant.

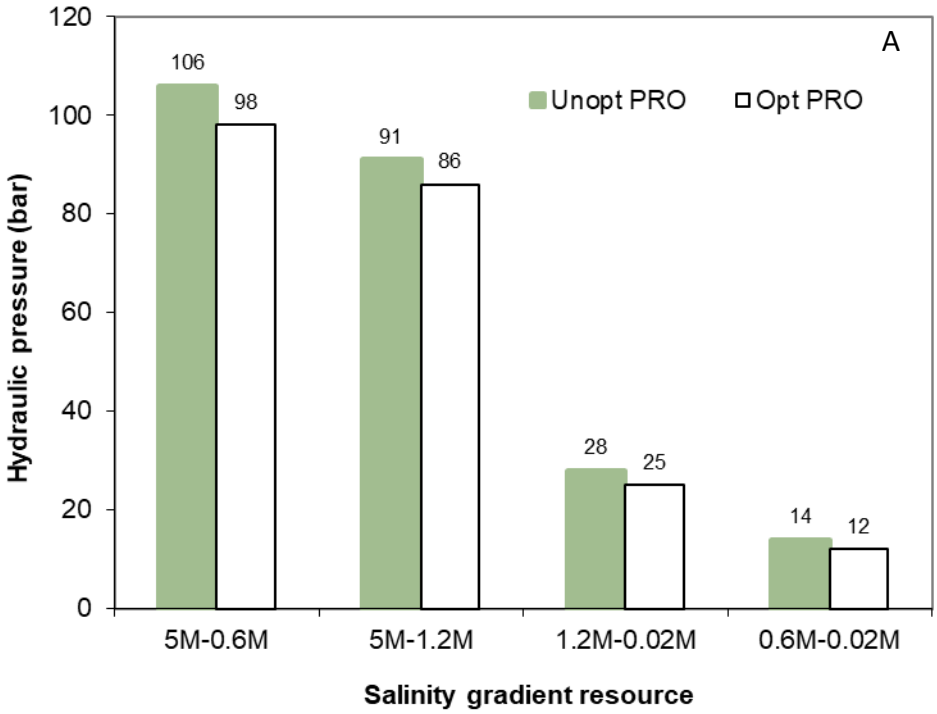

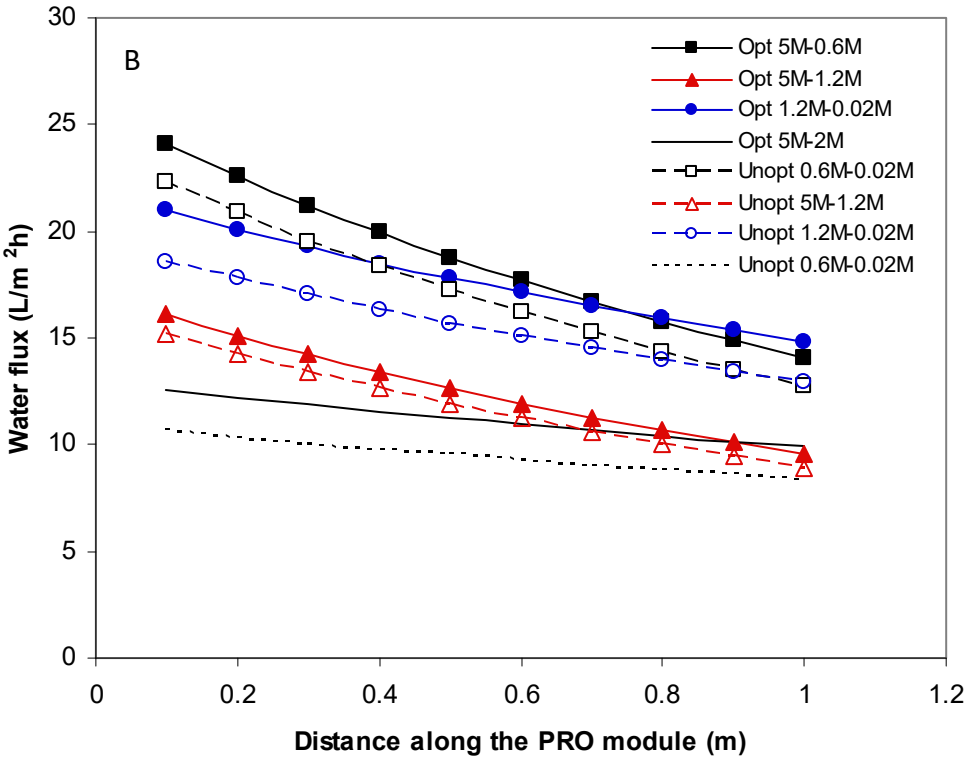

224

225

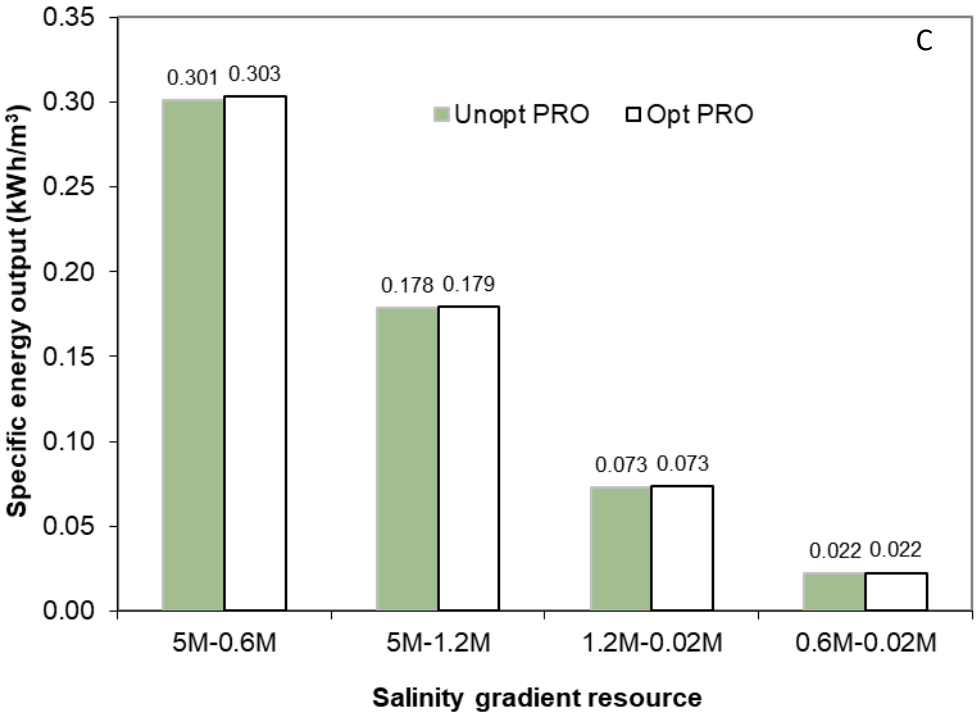

226

227

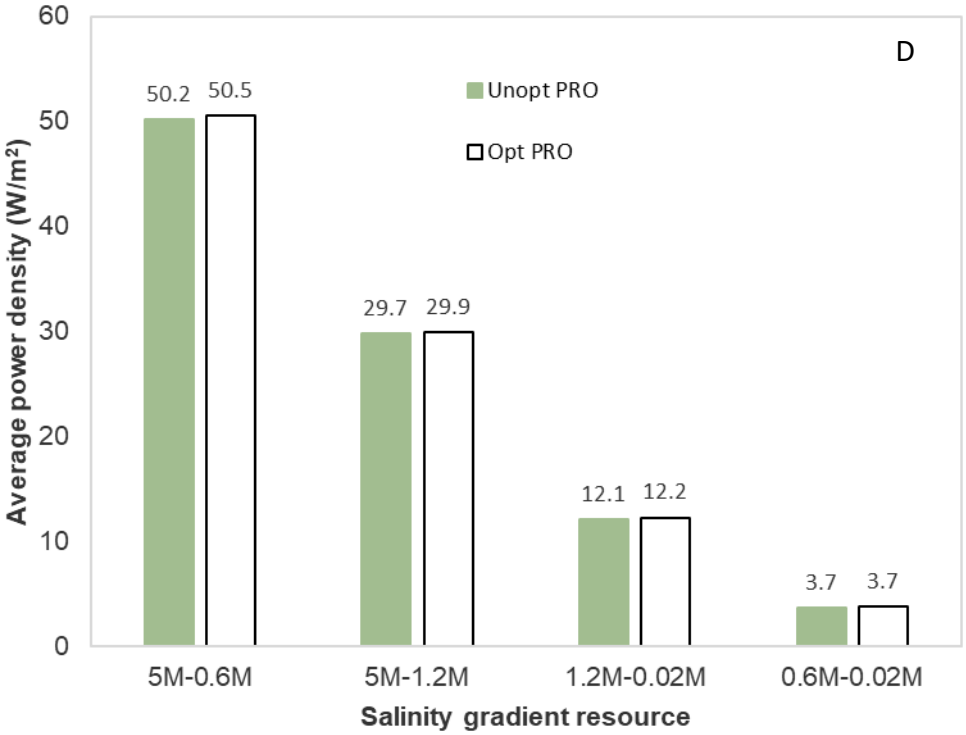

Figure 2: Results of the optimization analysis of applied hydraulic pressure in terms of: A) optimal applied hydraulic pressure; B) water flux; C) specific energy output D) average power density

3.2. Optimization of draw solution to mixture ratio

In irreversible PRO processes, researchers proposed that the optimum ration of draw to feed solution is 1:1 (i.e. draw to mixture ratio λ_D=0.5) at a hydraulic pressure equal to $\Delta P = \Delta\pi / 2$, which maximise the energy output achieved [4]. We performed an optimization analysis of draw solution flow rate at $\Delta P = \Delta\pi / 2$ for a number of salinity gradients [Figure 3]. Apparently, optimized PRO process requires γ_D values below 0.5, contrarily to what is recommended in earlier studies [Figure 3A]. In fact, the optimum γ_D was 0.35, 0.33, 0.31, and 0.26 for 5M-0.6M, 5M-1.2M, 1.2M-0.02M and 0.6M-0.02M salinity gradients, respectively. This suggests that γ_D decreased with decreasing the osmotic pressure gradient of the salinity gradient resource. In effect, decreasing the osmotic pressure gradient across the membrane results in a lower permeation flow and dilution of the draw solution. As such, the concentrative concentration polarization (ECP) on the feed side will be lower and the flow rate of the draw solution can be decreased. Finally, a direct effect of reducing γ_D on the energy generation is related to the definition of Es, in which a reduction in the flow rate of feed and/or draw solutions leads to an increase in the specific energy generation, though a reduction in the total generated power is expected as commented below [Figure 3D].

Water flux in optimized and unoptimized PRO process is shown in Figure 3B. Results show also in this case a decrease in water flux along the PRO module due to the

decrease in osmotic pressure driving force across the membrane [Figure 3B]. Water flux in the optimized and unoptimized PRO process was not changed for 5M-0.6M salinity gradient. For the other salinity gradients considered, optimized PRO process presents lower water flux than unoptimized water flux. This was due to the intensive concentration polarization at the draw solution side, because of the lower flow rate compared to unoptimized PRO process, in addition to the larger concentration variation due to a more intense dilution process in the smaller draw solution volume flowing in the channel. On the other hand, specific energy output was higher in the optimized PRO process than in the unoptimized process, this observation holds true for all salinity gradients. Despite the lower water flux in unoptimized PRO process, specific energy output was higher because of the lower draw solution flow rate according to Equation 4. The highest increase in specific energy output was 23% for 0.6M-0.02M salinity gradient followed by 14%, 13% and 10% for 1.2M-0.02M, 5M-1.2M and 5M-0.6M salinity gradient, respectively. Figure 3D reveals that the average power density in the optimized PRO process is equal to that in the unoptimized process in 5M-0.6M salinity gradient resource but it is lower than the average power density in unoptimized PRO process in 5M-1.2M, 1.2M-0.02M and 0.6M-0.02M salinity gradients. That is because reducing the flow rate in the optimized PRO process [Figure 3A] resulted in a decrease in the water flux across the membrane due to the effect of concentration polarization. Therefore, the average power density was lower in the optimized PRO process.

Overall, results show that optimization of the draw solution flow rate has more impact on improving the specific energy output in the PRO process. In fact, optimization of feed pressure resulted in a subtle increase of the specific energy output, <1%, while optimization of draw solution flow rate increased the specific energy output up to 23%. Moreover, a lower draw solution flow rate in real PRO plants would also decrease the effect of pumping losses on the overall process efficiency.

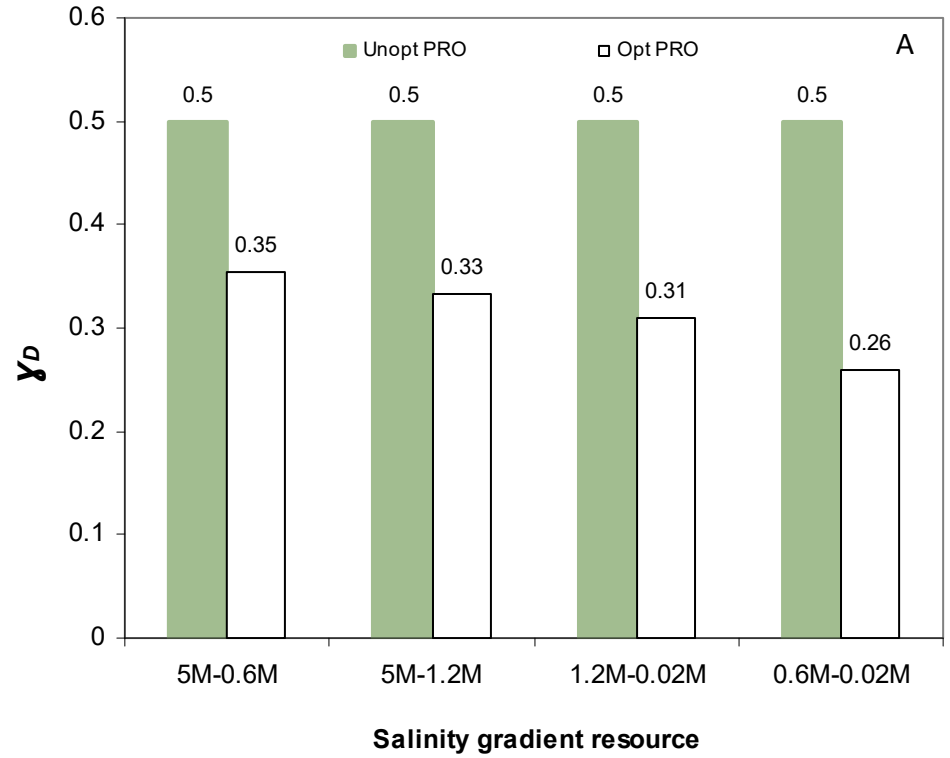

284
285
286

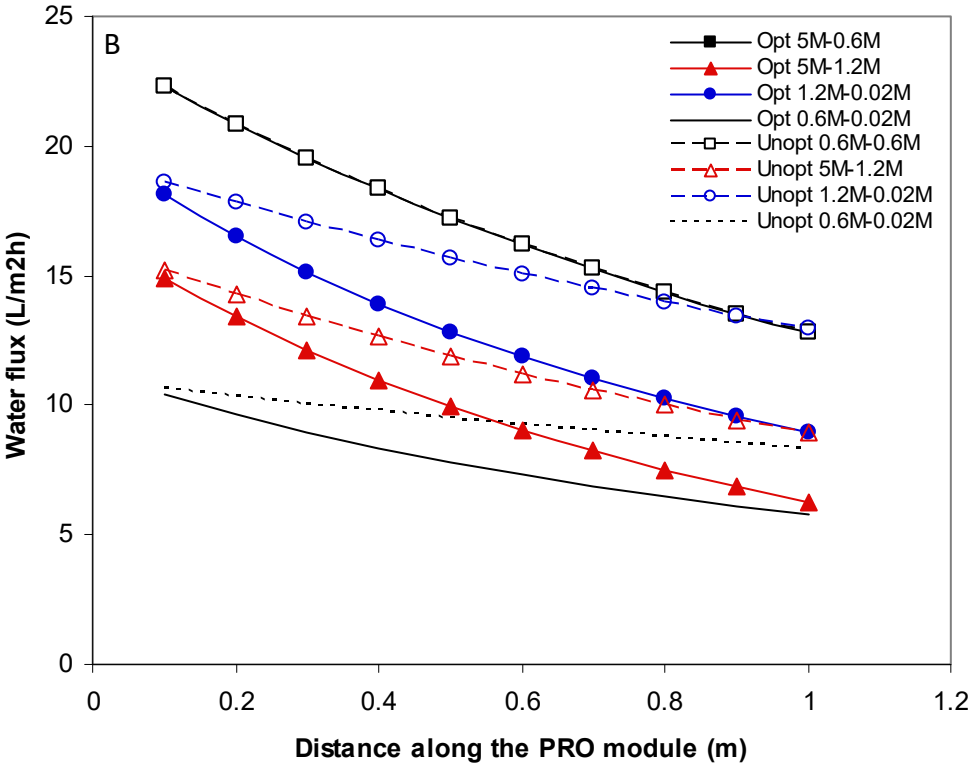

287
288

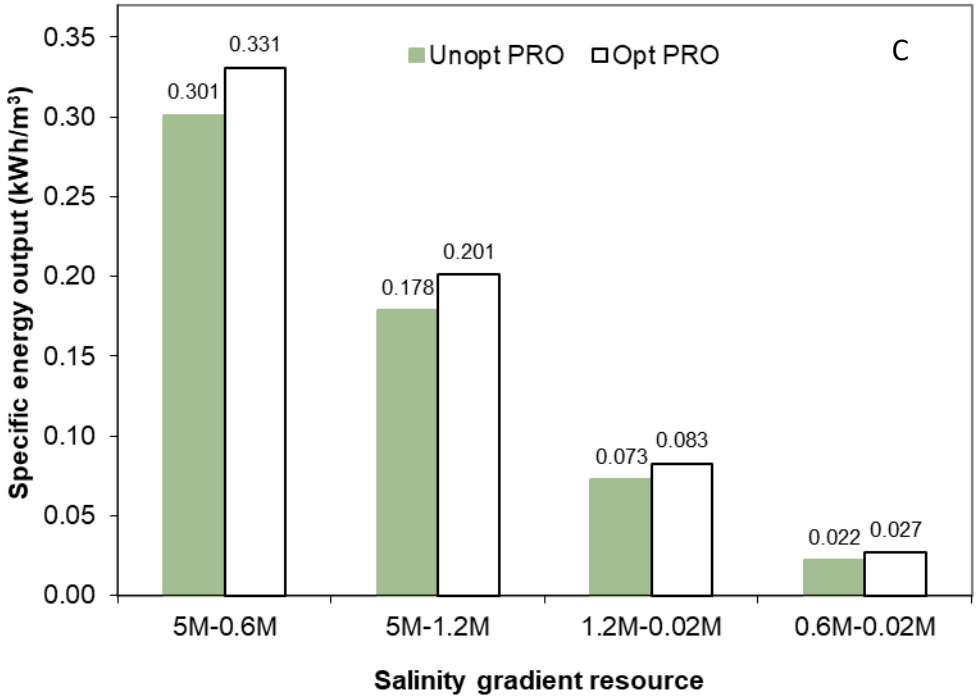

289

290

291

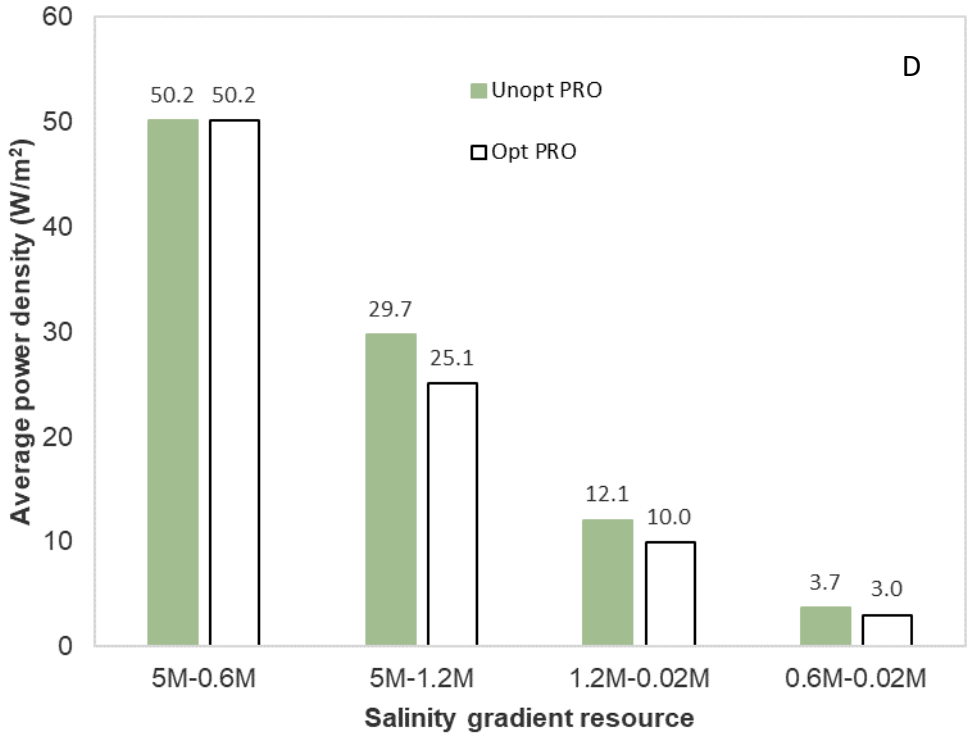

292

293 Figure 3: Results of the optimisation analysis of draw solution flow rate in terms of: A)
294 optimal draw solution mixing ratio; B) water flux; C) specific energy output; D)
295 average power density. Hydraulic pressure on the draw solution is equal to $\Delta\pi/2$

3.3. Optimization of feed solution to mixture ratio

Optimization of the feed solution to mixture ratio was carried out for the same salinity gradient resources previously considered and results were compared with the unoptimized cases. All results were obtained at a hydraulic pressure gradient equal to $\Delta P = \Delta\pi / 2$. In all cases the optimal ratio of feed flow rate in the mixing solution, γ_F, was significantly lower than the optimum value recommended in earlier studies (equal to 50% [5]), ranging from 0.2 to 0.23, 0.09, and 0.09 for 5M-0.6M, 5M-1.2M, 1.2M-0.02M and 0.6M-0.02M salinity gradients, respectively [Figure 4A]. Water flux, however, decreased along the PRO module and was lower in the optimized PRO process than in the unoptimized processes [Figure 4B]. Difference between optimized and unoptimized water flux increased with the increase of the osmotic pressure driving force across the PRO membrane because lower feed flow rate brought about more intense internal concentration polarization and a more pronounced reduction in the salinity gradient along the channel, as in the case of γ_D optimisation. There was a 30% decrease in water flux for both 5M-0.6M and 5M-1.2M salinity gradients, 13% for 1.2M-0.02M salinity gradient and 10% for 0.6M-0.02M salinity gradient. Despite the lower water flux in the optimized PRO process, specific power generation was higher in optimized PRO than reference conditions [Figure 4C]. This was because of the higher energy generation per cubic meter of mixed solution generated in the optimized PRO process. The highest specific energy generation was 0.402 kWh/m^3 for a 5M-0.6M salinity gradient, followed by 0.229, 0.123, and 0.037 for 5M-1.2M, 1.2M-0.02M and 0.6M-0.02M salinity gradient resource, respectively.

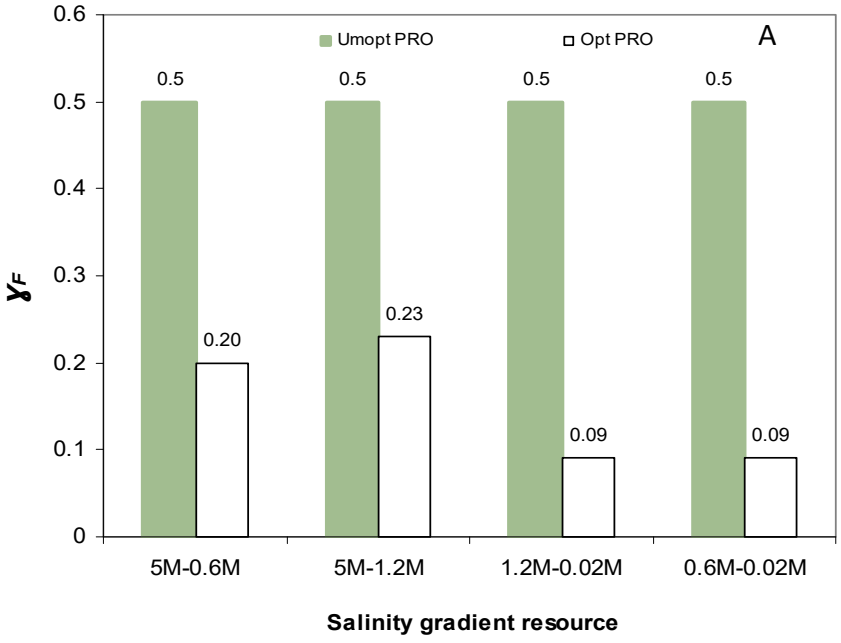

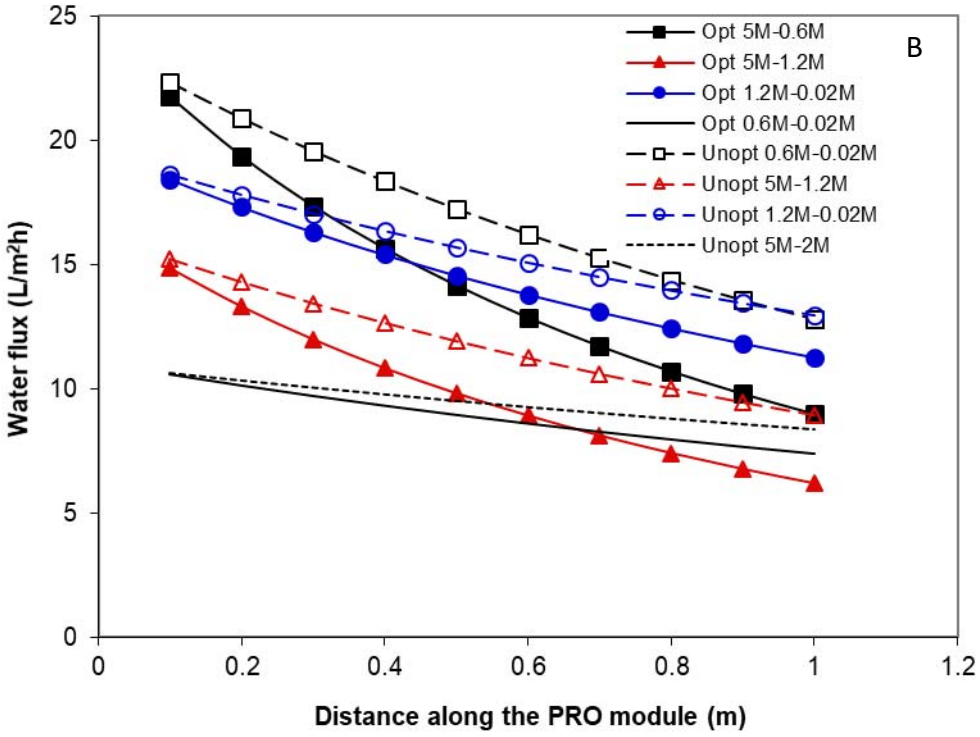
B
Opt 5M-0.6M
Opt 5M-1.2M
Opt 1.2M-0.02M
Opt 0.6M-0.02M
Unopt 0.6M-0.02M
Unopt 5M-1.2M
Unopt 1.2M-0.02M
Unopt 5M-2M
Water flux (L/m²h)
Distance along the PRO module (m)

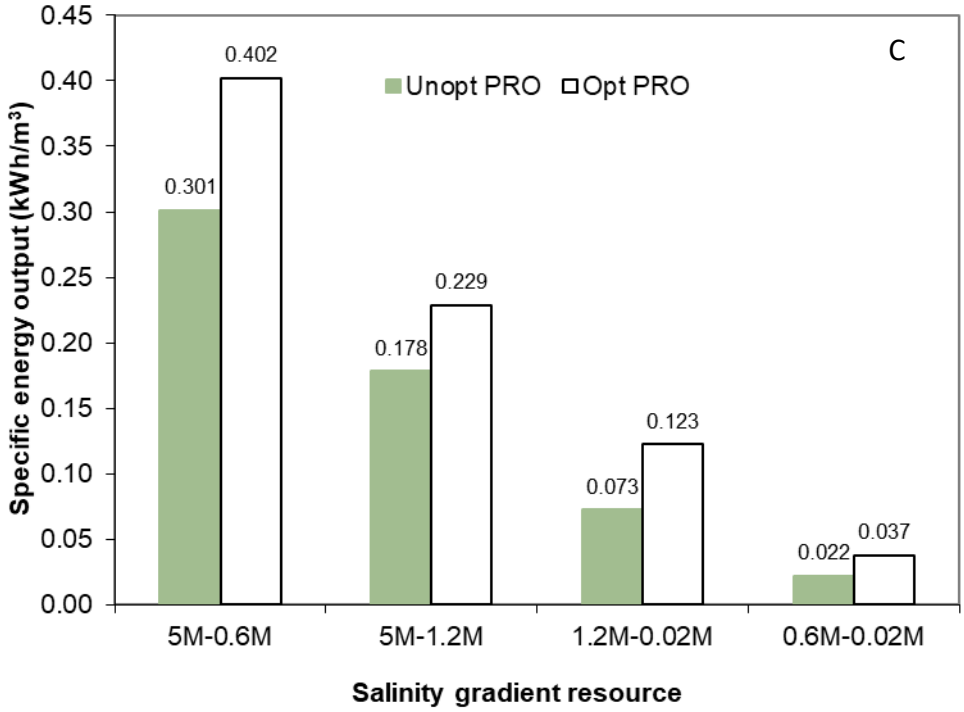
C
Unopt PRO
Opt PRO
0.301
0.402
0.178
0.229
0.073
0.123
0.022
0.037
Specific energy output (kWh/m³)
5M-0.6M
5M-1.2M
1.2M-0.02M
0.6M-0.02M
Salinity gradient resource

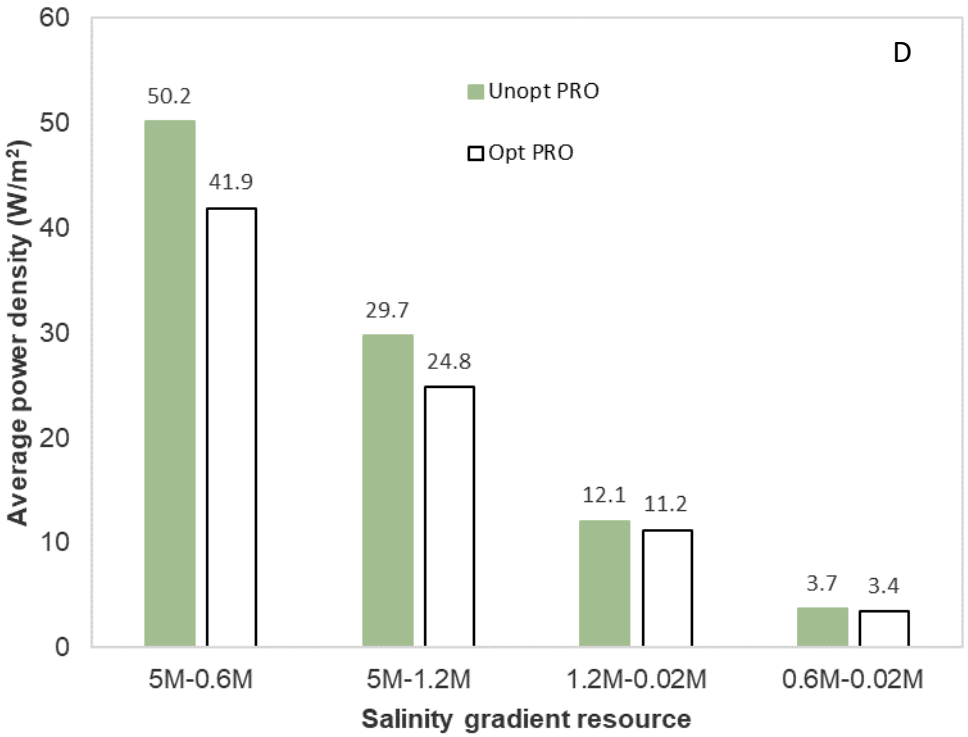

Figure 4: Optimization of feed solution flow rate A) optimized and unoptimized draw solution mixing ratio B) membrane flux C) energy output; D) average power density. Hydraulic pressure on the draw solution is equal to $\Delta\pi/2$

Results in Figures 4C and 4D show an improvement in the specific energy output in the optimized PRO process although the average power density in the optimized processes is lower than that in the unoptimized processes. The reason for this is that reducing the flow rate of draw solution reduced water flux and hence the average power density per square meter of membrane area. However, unoptimized PRO process uses higher draw solution flow rate and that decreased the specific energy output per cubic meter of processed draw and feed solution mixture, Equation [4]. This suggest that the average power density should not be always taken as an indicator for high performance PRO process as it does not consider the effect of feed and draw solution flow rates. Finally, feed flow optimization resulted in up to 68% increase in the specific energy generation for 0.6M-0.02M salinity gradient and about 65% increase in the specific energy generation for 1.2M-0.02M salinity gradient. Results also show that optimization of feed flow rate had the highest impact on the specific energy generation in the PRO process, followed by draw solution flow rate and finally the hydraulic pressure. It should be mentioned that although hydraulic pressure optimization resulted in subtle increase in the specific energy generation, it also allows PRO process to work at lower pressure, which may decrease the capital cost because of the less demanding high-pressure pump and PRO membrane specifications required.

3.4 Optimization of hydraulic pressure and feed flow rate

Simulation results revealed that optimization of feed flow rate results in a tangible improvement in the specific power generation in the PRO process. PRO process with optimized feed flow rate in section 3.3 was further optimized for the hydraulic pressure to improve the process performance. The combined effects of hydraulic pressure and feed flow rate on the performance of the PRO process is shown in Figure 5. The ratio of feed flow in mixture, γ_F, reduced from 0.5 in the unoptimized PRO process to 0.2 in the optimized PRO process using 5M-0.6M salinity gradient resource [Figure 5A]. Reducing the flow rate of feed solution will increase the specific energy generation according to Equation 4 while decreasing the operation and capital cost. For 5M-1.2M, 1.2M-0.02M and 0.6M-0.02M salinity gradients, γ_F was 0.23, 0.09 and 0.9 respectively. The ratio of feed flow rate to mixture in the optimized PRO process was between 18% and 46% of that in the unoptimized PRO process, γF ~0.5.

Water flux in the optimized and unoptimized PRO process is explained in Figure 5B. The optimized PRO process with 5M-0.6M and 5M-1.2M salinity gradients exhibited lower water flux than that in the unoptimized PRO process [Figure 5B]. This is caused by the lower feed flow rate in the optimized PRO process, which intensified the impact of concentrated concentrative concentration polarization. Water flux with the optimised PRO configuration follows the observed trend for the previous optimisation cases. In fact, while the reduction in the applied pressure leads to an increase in flux, the reduction of feed flow rate reduces it. The obtained trend of water flux along the channel indicates a significant reduction of water flux in the case of highly concentrated draw solutions (5M), with a maximum deviation between optimised and non-optimised case being around 30% in the last part of the channel. For lower concentration draw solution (1.2M and 0.6M) roughly the same average flux is observed for the optimised case. The difference in water flux between optimized and unoptimized PRO was 6% and 4% for 1.2M-0.02M and 0.6M-0.02M salinity gradients, respectively. The reason for insignificant difference in water flux between the optimized and unoptimized PRO process was due to low feed concentration, which caused only minor concentrative concentration polarization effect. Despite the lower water flux in the optimized PRO process, the specific power generation was higher in the optimized than in the unoptimized PRO process. This is due to the lower feed flow rate in the optimized PRO process, which resulted in a higher specific power output per mixed volume of salinity gradient resource. It should be mentioned that lower water flux in the optimized PRO processes indicates to the fact of larger membrane area is required to generate an equal flow comparing to unoptimized PRO process. In light of the results here, optimized PRO process requires between 4% to 29% higher membrane area. Although this will increase the capital cost, it should be noted that membrane life is 5 years at least. Furthermore, commercial PRO membranes price is now available as low as 17 USD/m2 such as Toyobo hollow fibre FO membrane [1]. For 1.2M-0.02M and 0.6M-0.02M salinity gradients, only 4% to 6% increase in the membrane area is required upon process optimization, which is insignificant difference over 5 years.

Specific power generation in the PRO process is illustrated in Figure 5C. The largest increase in the specific power generation was 72% in the optimized 0.6M-0.02M salinity gradient resource followed 1.2M-0.02M, 5M-0.6M, and 5M-1.2M salinity gradient, respectively [Figure 5C]. The lowest increase in the specific power generation was 29% for 5M-1.2M salinity gradient resource. This is probably due to the high feed concentration, which led to a significant concentrative concentration polarization. The average power density in the optimized PRO process was illustrated in Figure 5D. In general, the average power density in the optimized PRO process was lower than that in the unoptimized PRO process. The optimized resulted in a 16.3%, 16.1%, 6.6% and 5.4% reduction in the average power density for 5M-0.6M, 5M-1.2M, 1.2M-0.02M, and 0.6M-0.02M salinity gradient, respectively. All salinity gradient resources showed an average power density over 5W/m2 except 0.6M-0.02M salinity gradient in which it was 3.5 W/m^2. The optimum hydraulic pressure in the optimized POR process is 100, 89, 26, and 13 bar for 5M-1.2M, 1.2M-0.02M, and 0.6M-0.02M salinity gradient, respectively [Figure 5D]. The corresponding values in the unoptimized PRO process are 106, 91, 28, and 13 bar, respectively. The advantage of operating the PRO at lower hydraulic pressure will be reflected on the operation and capital cost of the PRO process that would need lower equipment specifications than the unoptimized PRO process.

The energy generation in the PRO module only is the difference between energy output and energy input [17]. The energy input, E_{in} (kWh/m^3), around the PRO module is the pumping energy that is calculated from the following expression:

$$E_{in} = \frac{Q_{Di} * P_F + Q_{Fi} * P_D}{n * Q_p} \quad [5]$$

Where, P_F and P_D are the pressure of feed and draw solution (bar), Q_P is the permeate flow rate and n is the pump efficiency. The energy required for pumping solution in the PRO module is 1 bar [17]. The net energy generation in the PRO process depends on the type of salinity gradient resource and are illustrated in table1 for the analysed scenarios. The results show that highest net energy output was 0.313 kWh/m^3 for 5M-0.6M salinity gradient resource followed by 5M-1.2M salinity gradient resource (0.095 kWh/m^3) and 1.2M-0.02M salinity gradient resource (0.036 kWh/m^3). For 0.6M-0.02M salinity gradient resource, the energy output was lower than the energy input as illustrated in Table 1. In effect, the energy output in the PRO process is directly dependent on the chemical potential of salinity gradient resource. Unfortunately, 0.6M-0.02M salinity gradient has low chemical potential, which resulted in an insignificant driving force across the membrane to generate enough osmotic power. The results of this study is in agreement with previous findings, which highlighted significance of salinity gradient for power generation in the PRO process [5, 18]. Apparently, salinity gradient with low osmotic energy such as 0.6M-0.02M salinity gradient is not suitable for power generation in the PRO process unless significant improvements in the process are achieved (e.g. increasing the water permeability of PRO membrane or dramatically reducing the pumping losses in the PRO module). On the other hand, the energy generated from 5M-0.6M, 5M-1,2M and 12M-0.02M salinity gradients was promising for power generation from osmotic energy. More research is underway to develop high permeability PRO membrane and better performing modules but one of the major issues to overcome is the membrane cost.

453

454

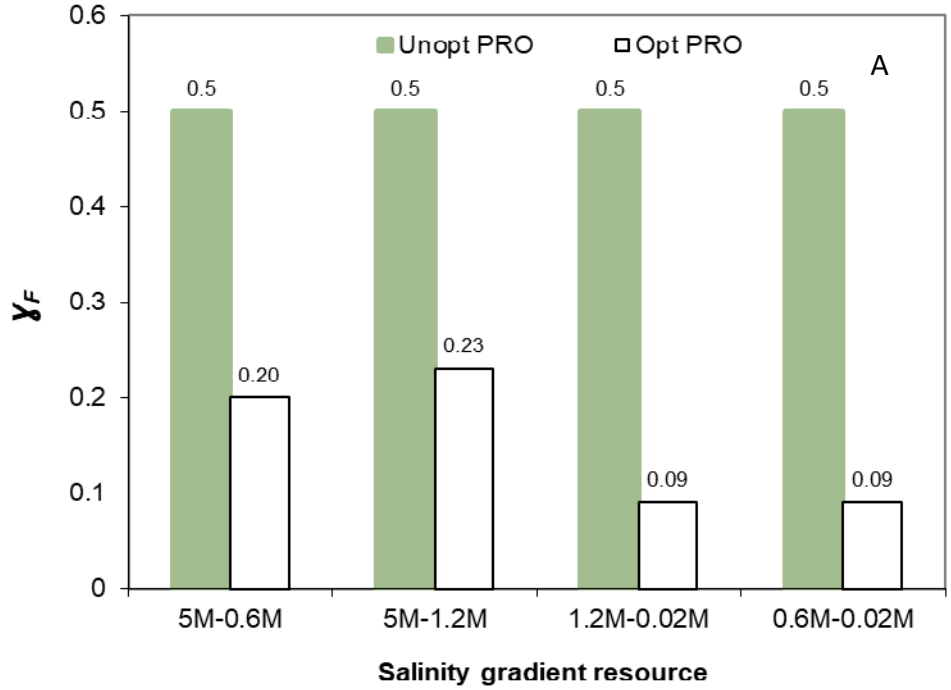

455
456
457

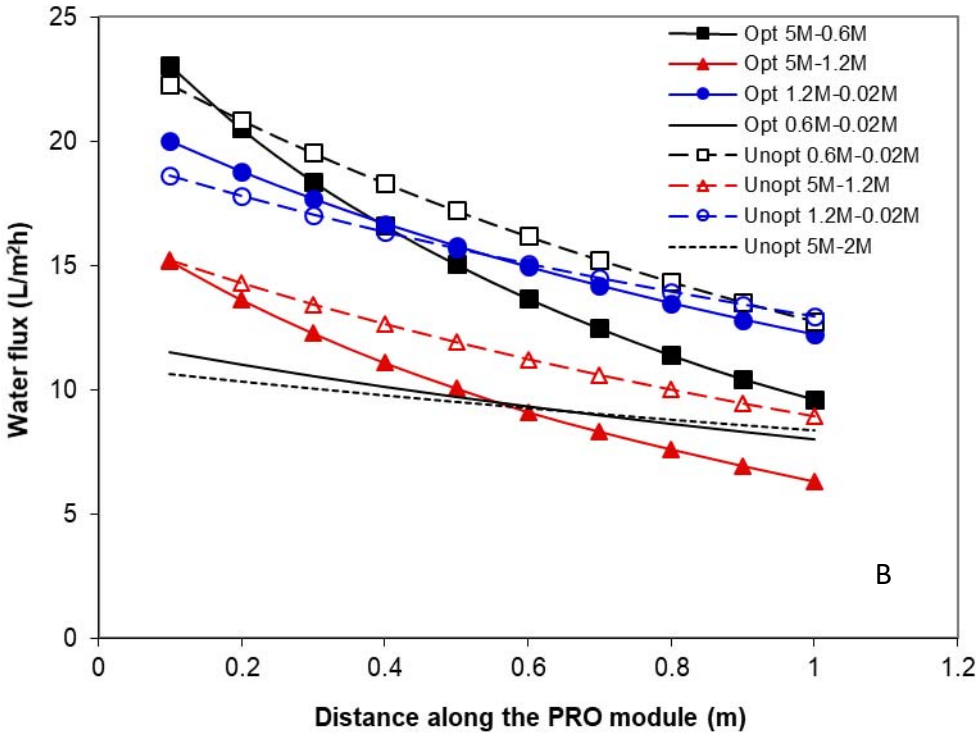

458
459
460

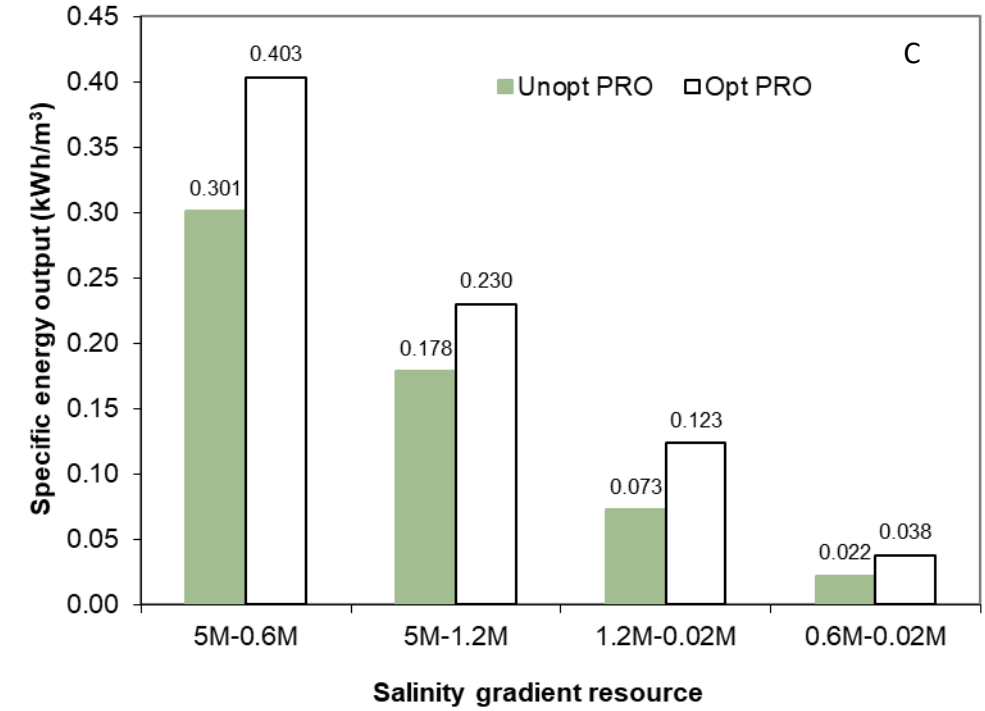

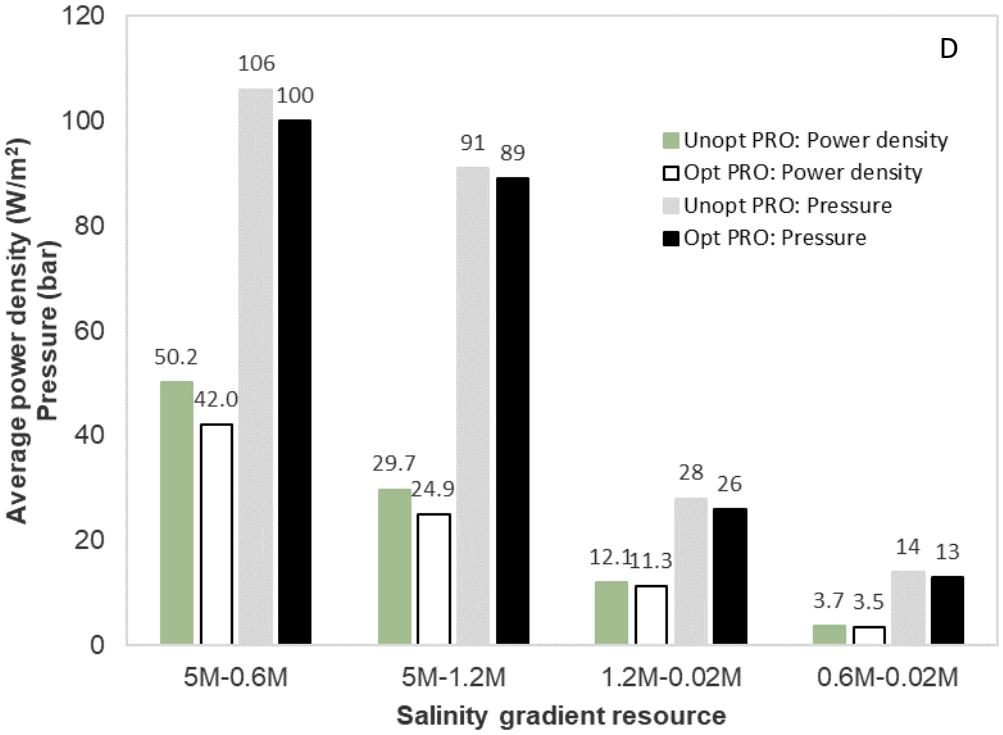

Figure 5: Optimized hydraulic pressure and feed flow rate in PRO A) feed flow fraction in mixture B) water flux C) specific power consumption D) average average power density.

Table 1: Net energy generation in the PRO process for different salinity gradient resources as the difference between the energy generation and pumping energy in the PRO module

	Energy kWh/m^3			
Process Description	**5M-0.6M**	**5M-1.2M**	**1.2M-0.02M**	**0.6M-0.02M**
Pumping energy in module	0.090	0.135	0.087	0.141
Energy output	0.403	0.230	0.123	0.038
Net energy input	**0.313**	**0.095**	**0.036**	**-**
Applied Pressure bar (opt)	*100*	*89*	*26*	*13*

4. Conclusions

PRO process was evaluated for power generation from salinity gradient resources under different operating conditions. Key operating parameters such as the hydraulic pressure and feed and draw fractions in the mixing solution were optimized using a computer model. The results showed that the specific energy output of a full-scale PRO process could be increased by process optimization. Previous optimization processes performed in a laboratory size experimented ignored the impact of draw solution dilution along the PRO module. The results of this study showed that dilution of draw solution in a full-scale module has significant impact on the operating parameters. This is due to the change in the chemical potential and osmotic energy along the PRO module in the PRO process. The key operating parameters in laboratory size experiment, $Q_D=Q_F$ and $\Delta P=\Delta\pi/2$, was found invalid in a full-scale PRO module.

The impact of the optimized operating parameters on the energy output in the PRO process varied from a subtle to a tangible increase in the specific energy generation. Hydraulic pressure was found to have a subtle impact on the energy output in the PRO process, <5% increase in the energy output, while the optimization of draw solution flow rate brought out up to 23% increase in the energy yield. However, optimization of the feed flow rate demonstrated the highest impact on the energy yield in the PRO process with up to 68% increase. Finally, PRO process was optimized for the hydraulic pressure and feed flow rate to maximize the specific energy generation in the PRO process. The study showed the importance of computer-based algorithms in engineering and renewable energy field.

Appendix

A1 Model description

Equation 1 calculates water flux, J_w, in the PRO process [21]:

$$J_w = A_w\left(\frac{\pi_{Db}e^{\left(\frac{-J_w}{k}\right)} - \pi_{Fb}e^{(J_wK)}}{1+\frac{B}{J_w}(e^{(J_wK)} - e^{\left(\frac{-J_w}{k}\right)})} - \Delta P\right) \quad [1]$$

where, π_{Db} and π_{Fb} are the osmotic pressures of the bulk draw and feed solution, respectively, A_w is the water permeability coefficient, ΔP is the hydraulic pressure across the PRO membrane, k is the mass transfer coefficient, B is the solute permeability coefficient, and K is the solute resistivity for diffusion within the porous support layer. The bulk concentration of draw solution, C_{Db}, is the average of inlet and outlet concentration of draw solution. We assumed PRO module of L length and divided into x number of equal sections. Equation 2 calculated the bulk concentration of draw solution, C_{Db-x}, at distance x from the membrane inlet:

$$C_{Db,x} = \frac{C_{Di,x}+C_{Do,x}}{2} \quad [2]$$

where, $C_{Di,x}$ and $C_{Do,x}$ are the inlet and the outlet concentrations of the draw solution at distance x. We assumed a PRO membrane of a perfect rejection to solutes, the outlet concentration of draw solution can be determined from mass and flow balance equation. At the entrance of the PRO module, the inlet concentration of draw solution; is already known whereas the outlet concentration of draw solution is obtained from mass and flow balance of draw solution [22]:

$$C_{Do,x} = \frac{C_{Di,x}*Q_{Di,x}}{D_{Do,x}} \quad [3]$$

where, Q_{Di-x} is the inlet flow rate of draw solution, C_{Di-x} is the inlet concentration of draw and Q_{Do-x} is the outlet flow rate of draw solution. The calculated output parameters from the previous section will be the input parameters of the next section. Furthermore, Q_{Do-x} is the sum of inlet flow rate of draw solution, Q_{Di-x}, and permeate flow rate, Q_{p-x}:

$$Q_{Do,x} = Q_{Di,x} - Q_{p,x} \quad [4]$$

Compensating equation 3 in Equation 2 to give:

$$C_{Db,x} = \frac{C_{Di,x}\left(1+\frac{Q_{Di,x}}{Q_{Do,x}}\right)}{2} \quad [5]$$

Similarly, the bulk concentration of feed solution, C_{Fb-x}, is calculated from averaging the inlet and outlet concentrations of feed solution as in Equation 6:

$$C_{Fb,x} = \frac{C_{Fi,x}+C_{Fo,x}}{2} \quad [6]$$

here, $C_{Fi\text{-}x}$ and $C_{Fo\text{-}x}$ are the concentrations of inlet and outlet feed solution. Equation 7 calculates the outlet concentration of feed solution form mass and flow balance at the draw solution side of the PRO membrane [2]:

$$C_{Fo,x} = \frac{C_{Fi,x} * Q_{Fi,x}}{Q_{Fo,x}} \quad [7]$$

where, $C_{Fi\text{-}x}$ is the feed solution inlet concentration, $Q_{Fi\text{-}x}$ is the inlet flow rate of feed solution and $Q_{Fo\text{-}x}$ is the outlet flow rate of feed solution. $Q_{Fo\text{-}x}$ is equal to the difference between $Q_{Fi\text{-}x}$ and $Q_{p\text{-}x}$. Compensating equation 7 in equation 6 gives:

$$C_{Fb,x} = \frac{C_{Fi,x}\left(1+\frac{Q_{Fi,x}}{Q_{Fo,x}}\right)}{2} \quad [8]$$

Equations 5 and 8 calculate the bulk concentration of draw and feed solutions respectively; substituting equations 5 and 8 in equation 1 and using Van't Hoff equation for the osmotic pressure calculation:

$$J_{w,x} = A_w\left\{\frac{\left(nRTC_{Di,x}\left(1+\frac{Q_{Di,x}}{Q_{Do,x}}\right)/2\right) exp\left(\frac{-J_{w,x}}{k_d}\right) - nRTC_{Fi,x}\left(1-\frac{Q_{Fi,x}}{Q_{Fo,x}}\right) exp\left(J_{w,x}K+\frac{J_{w,x}}{k_f}\right)}{1+\frac{B}{J_{w,x}}\left(exp\left(J_{w,x}\frac{J_{w,x}}{k_f}\right) - exp\left(\frac{-J_{w,x}}{k_d}\right)\right)} - \Delta P\right\} \quad [9]$$

More information about the model used in calculating water flux in the PRO process can be found in literature [17].

A2 Model validation:

The computer model used in this study was validated using pilot plant data [21]. The hollow fibre PRO membrane has water permeability coefficient equal to 0.27 L/m^{2}h.bar and membrane area equal to 70.5 m^2 and 1.M NaCl and DI water draw and feed solution, respectively. Water flux calculated from the computer model, $J_{w\text{-}m}$, was compared with the experimental flux, $J_{w\text{-}exp}$, data [Figure 5a-1, reference 21]. Different draw solution flow rate (Q_{DS}), feed solution flow rates (Q_{FS}), draw solution pressure (P_{DS}) and feed solution pressure (P_{FS}) are used in the model validation. According to Table A1, there are good agreement between theoretical and experimental data, over 90%.

Table A1: Experimental and theoretical water flux from the pilot plant test at different draw feed solution flow rates, Q_{DS} and Q_{FS} respectively. Membrane structure parameter 1024 µm and salt permeability coefficient 0.035 L/m^{2}h.

P_{DS} (bar)	P_{FS} (bar)	Q_{DS} (L/h)	Q_{FS} (L/h)	$J_{w\text{-}exp}$ (Lm^2/h)	$J_{w\text{-}m}$ (Lm^2/h)	%Agreement
5	2.8	480	480	6	5.65	94.2
8	3.1			5.5	5.27	95.8
11.8	3.2			4.9	4.73	96.5

14.6	3.3			4.5	4.36	96.9
16	3.5			3.9	4.2	92.9
21.5	3.7			3.5	3.46	98.9
24	3.8			3.2	3.17	99.1
27.5	4.1			2.8	2.75	98.2
30	4.2			2.6	2.45	94.2
6.3	4	480	600	6.2	5.64	91.0
13	4.5			4.9	4.78	97.6
16	4.7			4.6	4.35	94.6
17.8	4.8			4.2	4.13	98.3
26	5.3			3.3	3.11	94.2

Reference:

[1] Ali Altaee, Guillermo Zaragoza, Enrico Drioli, John Zouh, Evaluation the Potential and Energy Efficiency of Dual Stage Pressure Retarded Osmosis Process, Applied Energy, V 199 (2017), 359–369

[2] Arshian Sharif, Syed Ali Raza, Ilhan Ozturk, Sahar Afshan, The dynamic relationship of renewable and nonrenewable energy consumption with carbon emission: A global study with the application of heterogeneous panel estimations, Renewable Energy, V 133 ()2019, 685-691

[3] Stein Erik Skilhagen, Dr. Rolf Jarle Aaberg, Osmotic power - Power production based on the osmotic pressure difference between fresh water and sea water, Owemes 2006, 20-22 April. Citavecchia, Italy.

[4] A. Achilli, T. Y. Cath and A. E. Childress, Power generation with pressure retarded osmosis: An experimental and theoretical investigation, Journal of Membrane Science, V 343 (2009), 42–52

[5] S. Lin, A. P. Straub, M. Elimelech, Thermodynamic limits of extractable energy by pressure retarded osmosis, Energy Environmental Science, V 7 (2014), 2706–2714

[6] Jonathan Maisonneuve, Pragasen Pillay, Claude B. Laflamme, Pressure-retarded osmotic power system model considering non-ideal effects, Renewable Energy, V 75 (2015), 416-424

[7] Alexandros Daniilidis, David A. Vermaas, Rien Herber, Kitty Nijmeijer, Experimentally obtainable energy from mixing river water, seawater or brines with reverse electrodialysis, Renewable Energy, V 64 (2014), 123-131

[8] Fei Liu, Orlando Coronell, Douglas F. Call, Electricity generation using continuously recirculated flow electrodes in reverse electrodialysis, Journal of Power Sources, V 355 (2017), 206-210

[9] Masaru Kurihara, Masayuki Hanakawa, Mega-ton Water System: Japanese national research and development project on seawater desalination and wastewater reclamation, Desalination, Volume 308 (2013), 131-137

[10] Keiichiro Saito, Morihiro Irie, Shintaro Zaitsu, Hideyuki Sakai, Hidechito Hayashi & Akihiko Tanioka, Power generation with salinity gradient by pressure retarded osmosis using concentrated brine from SWRO system and treated sewage as pure water, Desalination and Water Treatment, V 41 (2012), 114-121.

[11] Henrik T.Madsen, Steen Søndergaard Nissen, JensMuffc, Erik G.Søgaard, Pressure retarded osmosis from hypersaline solutions: Investigating commercial FO membranes at high pressures, Desalination, Volume 420 (2017), 183-190
[12] Ye Li, Shanshan Zhao, Laurentia Setiawan, Lizhi Zhang, Rong Wang, Integral hollow fiber membrane with chemical cross-linking for pressure retarded osmosis operated in the orientation of active layer facing feed solution, Journal of Membrane Science, Volume 550 (2018), 163-172
[13] Chun Feng Wan, Tianshi Yang, Wenxiao Gai, Yu De Lee, Tai-Shung Chung, Thin-film composite hollow fiber membrane with inorganic salt additives for high mechanical strength and high average power density for pressure-retarded osmosis Journal of Membrane Science, Available online 26 March 2018.
[14] Ye Li, Rong Wang, Saren Qi, Chuyang Tang, Structural stability and mass transfer properties of pressure retarded osmosis (PRO) membrane under high operating pressures, Journal of Membrane Science, Volume 488 (2015),143-153.
[15] Yunfeng Chen, Laurentia Setiawan, Shuren Chou, Xiao Hu, Rong Wang, Identification of safe and stable operation conditions for pressure retarded osmosis with high performance hollow fiber membrane, Journal of Membrane Science, Volume 503 (2016), 90-100.
[16] Kerri L. Hickenbottom, Johan Vanneste, Menachem Elimelech, Tzahi Y. Cath, Assessing the current state of commercially available membranes and spacers for energy production with pressure retarded osmosis, Desalination, Volume 389 (2016), 108-118
[17] Ali Altaee, John Zhou, Adnan Alhathal Alanezi, Guillermo Zaragoza, Pressure retarded osmosis process for power generation: Feasibility, energy balance and controlling parameters, Applied Energy, V 206 (2017), 303-311
[18] Tamburini A., Giacalone F., Cipollina A., Grisafi F., Vella G., Micale G., Pressure Retarded Osmosis: a membrane Process for Environmental Sustainability, Chemical Engineering Transactions, Vol. 47, 2016: 355-360.
[19] Ali Altaee, Graeme Millar, Guillermo Zaragoza, Integration and Optimization of Pressure Retarded Osmosis with Reverse Osmosis for Power Generation and High Efficiency Desalination, Energy, V 103 (2016), 110-118
[20] Yasuhiko Tanaka, Masahiro Yasukawa, Shohei Goda, Hidehiko Sakurai, Masafumi Shibuya, Tomoki Takahashi, Michimasa Kishimoto, Mitsuru Higa, Hideto Matsuyama, Experimental and simulation studies of two types of 5-inch scale hollow fiber membrane modules for pressure-retarded osmosis, Desalination, Volume 447 (2018), 133-146.
[21] Y. C. Kim, M. Elimelech, Potential of osmotic power generation by pressure retarded osmosis using seawater as feed solution: Analysis and experiments, Journal of Membrane Science, V 429 (2013), 330-337.
[22] A. Altaee, G. Zaragoza, A. Sharif, Pressure retarded osmosis for power generation and seawater desalination: Performance analysis, Desalination, V 344 (2014), 108-115